Radiation Chemistry of Alternative Fuel Oxygenates: Substituted Ethers

Stephen P. Mezyk* and William J. Cooper

Department of Chemistry, University of North Carolina at Wilmington, 601 S. College Road, Wilmington, North Carolina 28403

David M. Bartels

Chemistry Division, Argonne National Laboratory, Argonne, Illinois 60439

Kevin E. O'Shea and Taixing Wu

Department of Chemistry, Florida International University, Miami, Florida 33199

Received: October 20, 2000; In Final Form: December 22, 2000

Absolute rate constants for the reaction of ethyl *tert*-butyl, diisopropyl, and methyl *tert*-amyl ethers with the hydroxyl radical, hydrated electron, and hydrogen atom in water have been determined using electron pulse radiolysis (e_{aq}^- and •OH), absorption spectroscopy (e_{aq}^- and •OH), and EPR free induction decay attenuation (•H) measurements. At room temperature the hydroxyl radical reaction was found to be the primary loss pathway, with rate constants of $(1.81 \pm 0.09) \times 10^9$, $(2.49 \pm 0.12) \times 10^9$, and $(2.37 \pm 0.12) \times 10^9$ dm^3 mol^{-1} s^{-1} determined for these ethers, respectively. The reaction of the hydrated electron with these compounds was not significant, with upper limit values of $\leq 10^7$, $\leq 6.7 \times 10^6$, and $\leq 4.0 \times 10^6$ dm^3 mol^{-1} s^{-1} determined. The corresponding rate constants for hydrogen atom reaction with these ethers were $(7.04 \pm 0.11) \times 10^6$, $(6.70 \pm 0.09) \times 10^7$, and $(3.09 \pm 0.09) \times 10^6$ dm^3 mol^{-1} s^{-1}. On the basis of these rate constant values, the kinetic computer modeling of the free-radical removal of these ethers from N_2O-saturated aqueous solution was found to be in very good agreement with experimental steady-state, ^{60}Co, irradiation measurements.

Introduction

Since the U.S. phaseout of tetraethyllead in the 1970s, ever-increasing amounts of high-octane compounds, notably methyl *tert*-butyl ether (MTBE), have been added to gasoline to give cleaner burning fuel with reduced vehicle exhaust emissions.[1] However, the 1990 Clean Air Act (CAA) oxygenate requirements led refiners to more than double the amount of oxygenate being blended into gasoline, and this combination of large-scale use, high water solubility,[2] low soil adsorption (K_{oc} value),[3] and only minor biodegradability under normal aquifer conditions[2,4,5] has now resulted in large-scale MTBE contamination occurring in natural, ground, and drinking water systems. MTBE has very low odor and taste detection thresholds[6] and was classified as a suspect carcinogen by the Environmental Protection Agency (EPA) in 1996.

These problems have provided impetus within the petroleum industry to use more "environmentally friendly" fuel additives. The CAA requirements did not specify which oxygenates could be used as additives, and a number of oxygen-containing compounds, especially alcohols and ethers, have also been considered. In addition to MTBE, ethanol, *tert*-butyl alcohol (TBA), ethyl *tert*-butyl ether (ETBE), diisopropyl ether (DIPE) and *tert*-amyl methyl ether (TAME) have also been suggested.[1,7] While ethanol is a prime candidate for MTBE substitution, its use is not automatic: ethanol has a higher vapor pressure than MTBE, and thus addition of ethanol would require removal of some clean-burning hydrocarbons in order to achieve gasoline vapor pressure requirements. Also ethanol-blended gasolines pick up moisture in handling and storage, which could require that ethanol be handled and blended at distribution sites.[8] In contrast, the physical and chemical properties of the proposed alternative alkyl ether oxygenates show them to be similar to those of MTBE.[3]

The remediation of current oxygenate-contaminated ground and drinking water still remains a pressing environmental problem. Potential remediation technologies for MTBE-contaminated water have been reviewed,[2,6] and it has been shown that air stripping would not be a readily applicable technique because MTBE partitions substantially into water.[9] MTBE has only a moderate affinity for granulated activated carbon, and so adsorption onto carbon could be used for remediation of contaminated water in the concentration range 10−100 μg/L.[10] However, at higher contaminant concentrations advanced oxidation (and reduction) technologies (AOTs) are expected to be required. These technologies are defined as processes that use the hydroxyl radical (and hydrated electron) and include $H_2O_2/h\nu$, H_2O_2/Fe^{II}, H_2O_2/O_3, O_3, $TiO_2/h\nu$, sonolysis, and electron-beam treatment of contaminated waters.

Selection of the most appropriate and cost-effective remediation treatment often relies heavily on the predictions of computer models. Mathematical modeling can be performed at several different levels,[11] depending on the known chemistry, available computational resources, and the overall modeling objective. Kinetic models give the most information and provide the best test of the model against actual engineering data, because all defined or proposed chemistry in the system is

* To whom correspondence should be addressed. FAX: (910) 962-2410. E-mail: MezykS@uncwil.edu.

10.1021/jp003892y CCC: $20.00
Published on Web 03/09/2001

considered.[12] These kinetic models, however, are dependent on degradation mechanisms and accurate rate constant data being available.

Previously bimolecular rate constants and a mechanism for the electron-beam destruction of MTBE in aqueous solution have been reported.[13] In this work we have extended our kinetic study to the other potential fuel oxygenates, to determine the bimolecular rate constants for the reactions of ETBE, DIPE, and TAME with the hydroxyl radical, hydrogen atom, and solvated electron in aqueous solution at room temperature.

Experimental Section

The LINAC pulse radiolysis system at the Radiation Laboratory, University of Notre Dame, was used for determining the rate constants for the hydrated electron and hydroxyl radical reactions. This system has been described in detail previously.[14] The chemicals used in this study were obtained from Aldrich, except for *tert*-butyl alcohol (Fisher Scientific), and were of the highest purity available. All chemicals were used as received. Solutions were made immediately before irradiation, using water filtered by a Millipore Milli-Q system, which was constantly illuminated by a Xe lamp (172 nm) to keep organic contaminant concentrations below 13 ppb, as measured by an on-line TOC analyzer. All solutions were fully purged with high-purity N_2O or N_2 to remove dissolved oxygen. The ethers were also separately saturated with nitrogen.

During the irradiation process the solution vessels were bubbled with only the minimum amount of nitrogen necessary to prevent air ingress. The solution flow rates in these experiments were adjusted so that each irradiation was performed on a fresh solution. Dosimetry[15] was performed using N_2O-saturated, 10^{-2} mol dm^{-3} SCN^- solutions at $\lambda = 475$ nm, ($G\epsilon = 5.09 \times 10^4$) with average doses of 4−5 Gy per 2−3 ns pulse. Throughout this paper, G is defined as the number of species produced or destroyed per 100 eV and ϵ is in units of dm^3 mol^{-1} cm^{-1}.

The hydrogen atom reaction rate constant measurements were performed at Argonne National Laboratory using direct electron paramagnetic resonance (EPR) detection of the decay of the hydrogen atom in aqueous solution following pulse radiolysis.[16,17] The hydrogen atoms were generated in aqueous solution using 3 MeV electrons from a Van de Graaff accelerator. The established pulsed EPR-based free-induction-decay (FID) attenuation method was used, because it directly monitors the aqueous •H atom and gives simple pseudo-first-order kinetics.[18−22] This method involves a microwave probe pulse being applied to the sample immediately after irradiation, with the resulting FID of the •H atom low-field EPR line being recorded on a digital oscilloscope. Typically 500−2000 pulses were averaged to measure each FID trace, at a repetition rate of 120 Hz.

Stock acid (pH 2.0) solutions were obtained by the addition of $HClO_4$ to Millipore-filtered water. The recirculating system was completely filled with the stock solution (174 ± 1.0 mL), deoxygenated using argon, and then sealed. Scavenging experiments were then performed by successive injections of the liquid ethers. Accuracy of the ether concentrations in these experiments is estimated at better than 3%.

All pulse radiolysis experiments were performed at ambient temperature (22 ± 2 °C).

Steady-state radiolysis experiments were also performed at the Radiation Laboratory, utilizing their GammaCell ^{60}Co γ-source. These preliminary irradiations were separately performed for each ether at an initial concentration of 50.0 ppmw, using N_2O-saturated aqueous solutions (30.0 mL) in sealed vials (44.0 mL) at natural pH. The solution headspace was also flushed with N_2O gas prior to the irradiation. Irradiation times ranged from 0.5 to 28 min, at a dose rate of 212 Gy/min. Irradiated samples were kept at ice temperature until they were analyzed.

The ether concentration in all irradiated samples was determined by dual analysis, using a Hewlett-Packard (HP) 5890 Series II gas chromatograph equipped with two columns (Restek Corporation: Rtx BCA1, 0.53 mm i.d., 30 m; Rtx BCA2, 0.53 mm i.d., 30 m) in combination with a HP 19395A autosampler and a HP 3396 Series II integrator. Sample tray and column temperatures were held constant at 40 °C, while the loop connected autosampler and GC inlet was 60 °C. Calibration curves were determined from known concentrations of ether standards, using 2.5 mL volumes as samples for assay.

Results and Discussion

Hydrated Electron Rate Constants. The radiolysis of water produces hydroxyl radicals, hydrated electrons, and hydrogen atoms according to the stoichiometry[23]

$$H_2O \rightsquigarrow 2.7^{\bullet}OH + 2.6e_{aq}^- + 0.6{\bullet}H + 0.45H_2 + 0.7H_2O_2 + 2.6H^+ \quad (1)$$

where the numbers in this equation are the G values for the production of each species.

The solvated electron has an absorbance maximum at 800 nm, and rate constants for hydrated electron reaction with the three ethers were determined from the variation of the first-order absorbance decay rate at 700 nm, in nitrogen-saturated aqueous solutions at natural pH. These solutions also contained 0.50 mol dm^{-3} TBA used to scavenge hydroxyl radicals and hydrogen atoms. A Corning 3-71 cutoff filter was inserted in the analyzing light beam path to eliminate all light below 400 nm, and 10−20 pulses were typically averaged to obtain a single kinetic trace. A typical kinetic trace, for the reaction of the hydrated electron with 3.24×10^{-3} mol dm^{-3} TAME at natural pH, is shown in Figure 1a.

The rate of change of this absorption was not pure first order over its entire decay. There is some second-order component at shorter times so, to obtain only the pseudo-first-order rate constant, all of these electron absorption decays were fitted to the mixed-order decay equation[24]

$$[G\epsilon]_t = \frac{[G\epsilon]_0 k_3}{k_3 \exp(k_3 t) - 2k_4[G\epsilon]_0(1 - \exp(k_3 t))} \quad (2)$$

to derive the k_3 rate constant in the competition

$$e_{aq}^- + \text{TAME} \xrightarrow{k_3} \text{products} \quad (3)$$

$$2e_{aq}^- (+2H_2O) \xrightarrow{2k_4} 2OH^- + H_2 \quad (4)$$

where $2k_4 = 1.1 \times 10^{10}$ dm^3 mol^{-1} s^{-1}.[23] The solid line in Figure 1a corresponds to a fitted rate constant of $k_3 = (1.08 \pm 0.05) \times 10^5$ s^{-1}. By varying the concentration of TAME, the second-order plot shown in Figure 1b was obtained, giving a rate constant of $(3.97 \pm 0.78) \times 10^6$ dm^3 mol^{-1} s^{-1}. The relatively low rate constant for this highly reactive radical suggests that hydrated electron reaction with trace impurities (all ether purities determined by GC/MS to be ≥99%) could strongly influence the observed kinetics. Therefore, this measured rate constant can be considered as an upper limit, which

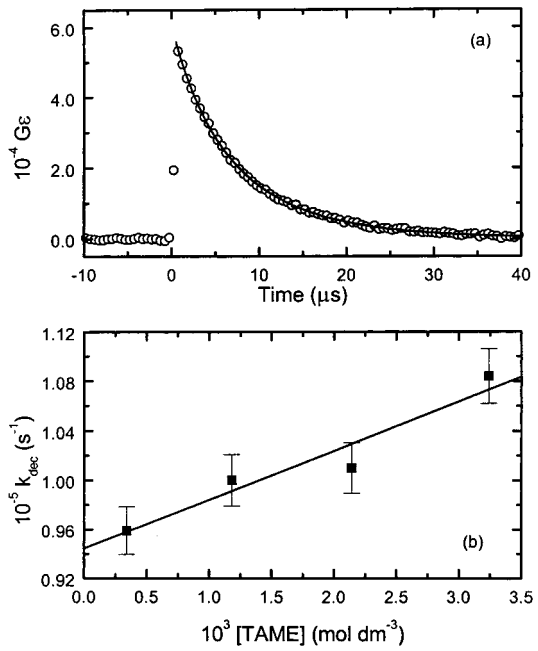

Figure 1. (a) Typical kinetic decay profile of the hydrated electron absorbance at 700 nm from pulse electron irradiated aqueous solution at natural pH containing 3.24×10^{-3} mol dm^{-3} TAME. The curve shown is the average of 10 pulses. The solid line corresponds to combined first- and second-order rate constant fitting (eq 2) with the pseudo-first-order value of $(1.08 \pm 0.05) \times 10^5$ s^{-1}. (b) Second-order rate constant determination for the reaction of the hydrated electron with TAME. Single-point error bars are one standard deviation, as determined from individual kinetic traces. The solid line corresponds to weighted linear fit, giving $k_3 = (3.97 \pm 0.78) \times 10^6$ dm^3 mol^{-1} s^{-1}.

TABLE 1: Summary of Bimolecular Reaction Rate Constants (dm^3 mol^{-1} s^{-1}) for Hydrated Electron, Hydrogen Atom, and Hydroxyl Radical Reactions with the Alternative Fuel Oxygenates Used in This Study in Comparison to Previous Literature Values

	e_{aq}^-	•H	•OH
DIPE	$\leq 6.7 \times 10^6$	$(6.70 \pm 0.09) \times 10^7$	$(2.49 \pm 0.04) \times 10^9$ $(3.7 \pm 0.4) \times 10^9$ [32]
ETBE	$\leq 10^7$	$(7.04 \pm 0.11) \times 10^6$	$(1.81 \pm 0.03) \times 10^9$ 3.2×10^9 [32]
TAME	$\leq 4.0 \times 10^6$	$(3.09 \pm 0.09) \times 10^6$	$(2.37 \pm 0.04) \times 10^9$

we take as $k_3 \leq 4.0 \times 10^6$ dm^3 mol^{-1} s^{-1}. This rate constant, along with all of the values determined in this study, is listed in Table 1.

Similar behavior was observed for hydrated electron reaction with DIPE in this study, with an upper limit rate constant of $\leq 6.7 \times 10^6$ dm^3 mol^{-1} s^{-1} determined.

However, for ETBE the measured second-order rate constant was significantly higher, $(8.74 \pm 0.21) \times 10^7$ dm^3 mol^{-1} s^{-1}. This factor of 10 increase over the other two ethers in this study suggested that impurity reactions were dominating the hydrated electron decay kinetics. The particular lot of ETBE used was 99.4% pure, with the remainder probably being a halide-containing compound (determined by inquiry to the chemical supplier). The reaction of such an impurity, with rate constant of $\sim 10^{10}$ dm^3 mol^{-1} s^{-1},[23] would readily account for much of the observed decay rate. Based on this, we believe that the hydrated electron reaction with ETBE would be of the same order of magnitude as the other two compounds determined in this study, and therefore assign an upper limit value of $\leq 10^7$ dm^3 mol^{-1} s^{-1}.

These upper limit rate constants for hydrated electron reaction are consistent with other values for analogous compounds in the literature: for example, for the reaction of hydrated electrons with diethyl ether a rate constant of $\leq 10^7$ dm^3 mol^{-1} s^{-1} was determined,[25] for MTBE, a value of $\leq 1.7 \times 10^7$ dm^3 mol^{-1} s^{-1} has been reported,[13] while for TBA, a value of $\leq 4 \times 10^5$ dm^3 mol^{-1} s^{-1} was found.[26]

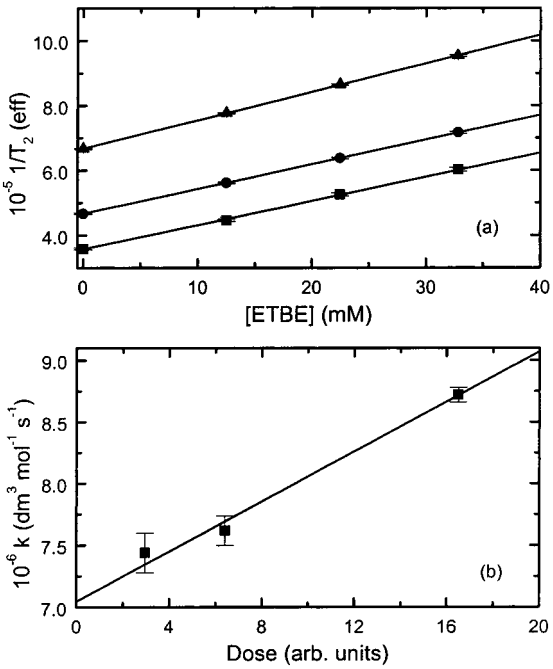

Figure 2. (a) Dose dependence of the hydrogen atom scavenging rate constants for ETBE at pH 2.0 and 21.6 °C. Solid lines correspond to fitted values of $(7.44 \pm 0.16) \times 10^6$ (■), $(7.62 \pm 0.12) \times 10^6$ (●), and $(8.72 \pm 0.06) \times 10^6$ (▲) dm^3 mol^{-1} s^{-1} for the 12, 25, and 55 ns pulse widths, respectively. (b) Rate constant extrapolation to "zero dose" for ETBE at pH 2.0 and 21.6 °C, to give a limiting value of $k_6 = (7.04 \pm 0.11) \times 10^6$ dm^3 mol^{-1} s^{-1}. Error bars correspond to one standard deviation obtained from weighted linear fits to the scavenging plots.

Hydrogen Atom Rate Constants. The overall hydrogen atom scavenging rate constants for these three ethers were determined using the FID-attenuation EPR methodology.[18−22] Measurements were performed at pH 2.0 to increase the initial yield of hydrogen atoms by conversion of the hydrated electrons:

$$e_{aq}^- + H^+ \rightarrow \bullet H \quad k = 2.3 \times 10^{10}\ dm^3\ mol^{-1}\ s^{-1}\ [23] \qquad (5)$$

The solutions also contained 1.0×10^{-2} mol dm^{-3} methanol to scavenge hydroxyl radicals.

In previous experiments using this technique, it was observed that the measured scavenging rate constants were slightly dependent on the dose used. The phenomenon was also found in the present study, as shown in Figure 2a for hydrogen atom reaction with ETBE at 21.6 °C. The general expression for the effective damping rate of the FID in these experiments is given by[18−20]

$$\frac{1}{T_2(\text{eff})} = \frac{1}{T_2^{\,o}} + k_6[S] + \sum k^i_{\text{ex}}[R_i] \qquad (6)$$

where k_6[S] is the •H atom scavenging rate for the reaction

$$\bullet H + R_2O \xrightarrow{k_6} \text{products} \qquad (7)$$

and $\sum k^i_{\text{ex}}[R_i]$ represents the spin-dephasing contribution of the second-order spin exchange and recombination reactions between •H atoms and other free radicals. The latter term in eq 6

is responsible for the shift in the intercept seen in Figure 2a, as the total free radical concentration $\sum[R_i]$ increases with the larger pulse sizes (doses) used. The scavenging reaction converts the hydrogen atoms into other free radicals, and the corresponding change in k^i_{ex} during the 5 μs experimental time period is responsible for the small changes in the slopes. The systematic error due to this second-order chemistry can be avoided either by working with a very small •H atom concentration, or by extrapolation to a "zero-dose" limit.

The technique used in this study was extrapolation to zero dose. The actual rate constants for hydrogen atom reaction with ETBE at this temperature, obtained from the second-order slopes of the data shown in Figure 2a, were $(7.44 \pm 0.16) \times 10^6$, $(7.62 \pm 0.12) \times 10^6$, and $(8.72 \pm 0.06) \times 10^6$ dm^3 mol^{-1} s^{-1} for the 12, 25, and 55 ns pulse widths, respectively. These pulses correspond to relative doses of 2.95, 6.40, and 16.5; these latter values were simply the measurements of the average beam current (μA) on a shutter positioned before the irradiation cell. These currents were assumed to be proportional to the actual dose given to the sample. The shutter beam current was monitored frequently to allow for any slight drift.

The extrapolation of these ETBE dose-dependent rate constants to zero dose is shown in Figure 2b. A good linear relationship is obtained, with a limiting, zero-dose, rate constant of $(7.04 \pm 0.11) \times 10^6$ dm^3 mol^{-1} s^{-1} calculated (see Table 1). Thermodynamic considerations suggest that the hydrogen atom reaction with ETBE would consist of abstraction of a hydrogen atom from the methylene group, to create a secondary carbon centered radical.

This limiting, zero-dose, value is consistent with previously reported rate constants for hydrogen atom reaction with analogous ethers in aqueous solution. For MTBE a rate constant of $(3.40 \pm 0.15) \times 10^6$ dm^3 mol^{-1} s^{-1} has been recently reported using this same EPR methodology.[13] This slower rate constant, which was believed due to hydrogen atom extraction from one of the terminal methyl groups, further supports the thermodynamic argument that methylene group hydrogen atom reaction dominates for ETBE. For diethyl ether, which has two methylene groups adjacent to the oxygen atom, a much faster •H atom reaction rate constant of 4.3×10^7 dm^3 mol^{-1} s^{-1} has been previously measured,[27] suggesting that in addition to the methylene hydrogen atom abstraction mechanism dominating, stabilization of the secondary carbon centered radical formed in diethyl ether also occurs.

Zero-dose hydrogen atom reaction rate constants for TAME and DIPE of $(3.09 \pm 0.09) \times 10^6$ and $(6.70 \pm 0.09) \times 10^7$ dm^3 mol^{-1} s^{-1}, respectively, were also determined in this study. The slower rate constant for hydrogen atom reaction with TAME suggests that the position (and hence activation) of methylene group hydrogen atoms is important; in TAME the methylene group is β to the oxygen atom and the lower rate constant is consistent with the expected lower C−H bond activation in this group. Conversely for DIPE, where abstraction of a hydrogen atom would result in a more stable tertiary carbon centered radical being formed, the hydrogen atom reaction rate constant is much faster.

Hydroxyl Radical Rate Constants. The reaction of hydroxyl radicals with the three ethers in this study did not show any significant intermediate species absorption. A typical transient spectrum is shown in Figure 3a, for a N_2O-saturated aqueous solution at natural pH containing 5.00×10^{-3} mol dm^{-3} DIPE. Only a weak increase in intensity at low wavelengths was seen, and this absorption intensity was too small to allow accurate direct measurements of the growth kinetics of this intermediate.

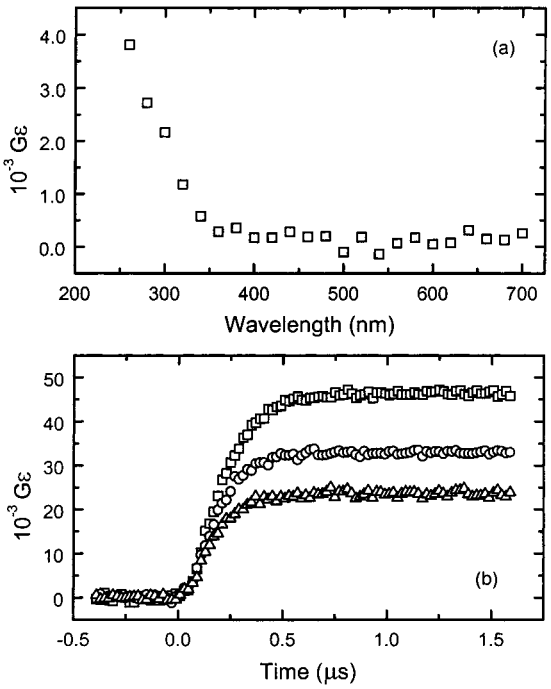

Figure 3. (a) Absorption spectrum of hydroxyl radical produced product observed in N_2O-saturated solution containing 5.00×10^{-3} mol dm^{-3} DIPE at 20.8 °C and natural pH. (b) Kinetics of $(SCN)_2^{\bullet-}$ formation at 472 nm for N_2O-saturated 9.81×10^{-4} mol dm^{-3} SCN^- containing zero (□), 1.90×10^{-3} (○), and 4.24×10^{-3} (△) mol dm^{-3} DIPE.

Therefore, hydroxyl radical rate constants for all three ethers were determined using competition kinetics, based on the competing reactions

$$\bullet OH + R_2O \xrightarrow{k_7} \text{products} \tag{8}$$

$$\bullet OH + SCN^- \xrightarrow{(+SCN^-)} (SCN)_2^{\bullet-} \tag{9}$$

When the ether reaction product does not absorb, this competition can be analyzed to give the following analytical expression:

$$\frac{[(SCN)_2^{\bullet-}]_0}{[(SCN)_2^{\bullet-}]} = 1 + \frac{k_8[R_2O]}{k_9[SCN^-]} \tag{10}$$

A plot of $[(SCN)_2^{\bullet-}]_0/[(SCN)_2^{\bullet-}]$ (or a ratio of parameters directly proportional to this ratio) against the ratio$[R_2O]/[SCN^-]$ gives a straight line of slope k_8/k_9. Based on the initial rate constant for hydroxyl radical reaction with SCN^-, $k_9 = 1.1 \times 10^{10}$ dm^3 mol^{-1} s^{-1},[23] the k_8 rate constant can be readily determined.

Typical kinetic data obtained at 472 nm are shown in Figure 3b. As expected, a decrease in the $(SCN)_2^{\bullet-}$ absorption intensity is observed when DIPE was added. However, it is important to note that analysis by eq 10 is only valid if the initial •OH concentration is the same for all conditions. Under our experimental conditions the added amounts of DIPE would cause an increase in the initial •OH concentration, due to intraspur scavenging. Therefore, this increase was also accounted for in the kinetics analysis using the established intraspur scavenging equations.[28−31] This correction was found to be on the order of the experimental error in these measurements.

Competition plots for DIPE and ETBE are shown in Figure 4, with derived rate constants of $(2.49 \pm 0.12) \times 10^9$ and (1.81

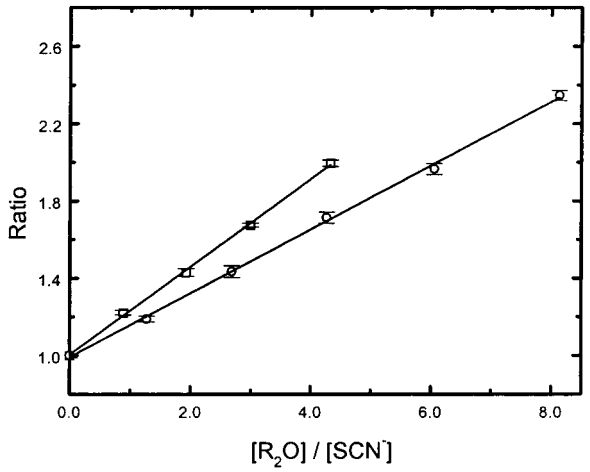

Figure 4. Initial yield corrected rate constant determination for hydroxyl radical reaction with the ethers (R_2O) DIPE (□) and ETBE (○). Error bars correspond to one standard deviation, as determined from individual yield measurements (cf. Figure 3b). Solid lines are weighted linear fits, with slopes of 0.226 ± 0.004 and 0.165 ± 0.003, respectively. These slopes give corresponding second-order rate constants for hydroxyl radical reaction with DIPE and ETBE as (2.49 ± 0.12) × 10^9 and (1.81 ± 0.09) × 10^9 dm^3 mol^{-1} s^{-1}.

± 0.09) × 10^9 dm^3 mol^{-1} s^{-1}, respectively. The data for TAME (not shown) gave (2.37 ± 0.12) × 10^9 dm^3 mol^{-1} s^{-1}.

Only one specific hydroxyl radical reaction rate constant has been previously reported in the literature for the three chemicals of this study. For DIPE thiocyanate competition kinetics were also used to determine a slightly higher rate constant of (3.7 ± 0.4) × 10^9 dm^3 mol^{-1} s^{-1}.[32] Two comparative values for hydroxyl radical reaction with MTBE have been reported, with rate constants of 1.6 × 10^9 [33] and 2.1 × 10^9 dm^3 mol^{-1} s^{-1},[13] again determined using SCN^- competition kinetics. There has also been one relative determination of the rate constant for hydroxyl radical reaction with ETBE in aqueous solution, where from steady-state ozone/hydrogen peroxide competition kinetics a rate constant ratio of $k_{OH+ETBE}/k_{OH+MTBE} \sim 1.7$ was obtained.[34] Taking an average of the two MTBE hydroxyl radical rate constants,[13,33] this gives a rate constant for hydroxyl radical reaction with ETBE of 3.2 × 10^9 dm^3 mol^{-1} s^{-1}, which is slightly higher, although within error, than the absolute value of (1.81 ± 0.09) × 10^9 dm^3 mol^{-1} s^{-1} obtained in this study. Rate constants for reaction of the hydroxyl radical with diethyl ether have also been previously determined using competition kinetics, with values of 2.9 × 10^9 (SCN^-)[32] and 4.2 × 10^9 (I^-)[35] dm^3 mol^{-1} s^{-1} reported. While the latter value appears to be somewhat high, the competitive SCN^- determination is in reasonable agreement with the three rate constants measured in this study.

The near equivalence of all these rate constants for hydroxyl radical reaction with these ethers in the aqueous phase is somewhat puzzling. Based on thermochemical bond strength considerations, one would again expect that the hydroxyl radicals would abstract a hydrogen atom from secondary or tertiary group carbons of these saturated ethers, where possible, and that as for •H atom reaction, the different reaction mechanisms and/or C−H bond activations due to proximity to the oxygen atom would be reflected in the observed rate constant. However, there is effectively no difference in the rate constant measured for aqueous MTBE[13] (H atom abstraction from primary methyl groups), ETBE, TAME, and diethyl ether[32] (abstraction from secondary methylene groups), or DIPE (abstraction from a tertiary carbon).

Insight into these rate constants, and the mechanism of reaction, was also sought from the greater body of gas-phase rate constant data. For oxygenated organic compounds a very good linear correlation between hydroxyl radical reaction rate constants in the gas and aqueous phases has been established,[36] and gas-phase values for hydroxyl radical reaction with most of the ethers of this study have been determined.[37−39] The measured gas-phase rate constants for ETBE and TAME were the same within error, which indicated that for the presumed hydrogen atom abstraction reaction there was no dependence on the proximity of the methylene group to the oxygen atom in these molecules, consistent with the aqueous rate constants measured in this study for these two ethers. However, the gas-phase rate constant for hydroxyl radical reaction with MTBE would predict that the aqueous value should be about a factor of 2−3 slower than for the methylene group containing ethers, not equal. In contrast, recent kinetic data reported[40] for chlorine atom reaction with ethers in the gas phase showed equivalent rate constants for reaction with MTBE, ETBE, and DIPE, but considerably enhanced reactivity for diethyl ether, in agreement with the aqueous •H atom rate constant measurements of this study, but not observed for hydroxyl radical reaction in the aqueous phase. Although no specific mechanism for chlorine atom reaction with these ethers was given,[40] hydrogen atom abstraction from the ethers appears to have been assumed: the overall rate constants were analyzed in terms of the specific reactivity of the $-CH_3$, $-CH_2-$, and $>CH-$ groups in these ethers, a product radical that could regenerate Cl atoms from Cl_2 was found, and there was a very good free-energy correlation of the measured rate constants with the gas-phase hydroxyl radical rate constants found for all ethers studied, except MTBE.

The disparity for MTBE in the correlation between the hydroxyl radical and chlorine atom rate constants in the gas phase suggests that there could be a different mechanism of reaction for this ether compared to those of this study. An enhanced rate constant in the solution phase, relative to the gas phase, is expected for species undergoing an initial hydroxyl radical addition reaction.[36] If such an addition reaction occurred for MTBE, then this enhancement could offset the expected lower aqueous rate constant, to give (fortuitous) agreement with the aqueous hydroxyl radical rate constants for the methylene group containing ethers, where reaction is expected to occur by direct hydrogen atom abstraction. These two reaction mechanisms can be differentiated in the gas phase by temperature-dependent rate constant measurements; the hydroxyl radical reaction by direct abstraction of a hydrogen atom from a methylene group has a slight positive temperature dependence, whereas the addition of a hydroxyl radical to a species shows a negative temperature dependence. Therefore, it would be very interesting to determine the temperature dependence of hydroxyl radical reactions in aqueous solution.

Steady-State Irradiation Measurements. The goal of this research was to obtain reaction rate constants for the reaction of hydroxyl radicals, hydrated electrons, and hydrogen atoms to be used in the construction of a kinetic/mechanistic model for the AOT-based destruction of these ethers in aqueous solution. Based on the measured rate constants and the radical production yields, in the electron beam remediation of these ethers the production of carbon-centered radicals by reaction of hydroxyl radicals is predicted to be the major process. To further support and verify our pulse radiolysis rate constant measurements, steady-state radiolysis experiments were also performed in this study. These steady-state measurements were

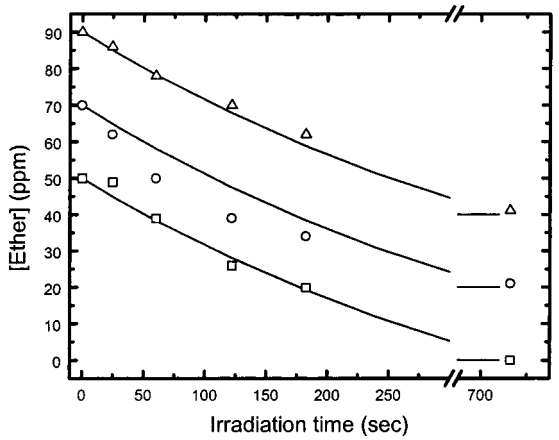

Figure 5. Variation in ETBE (□), DIPE (○), and TAME (△) concentration with increasing steady-state ^{60}Co irradiation (3.54 Gy/s) of aqueous ether solutions. All ether concentrations were initially 50.0 ppmw in 30.0 mL of N_2O-saturated solution at natural pH. Plotted data for DIPE and TAME offset by +20 and +40 ppmw, respectively, for clarity. Solid lines correspond to kinetic computer modeling predictions for ether removal, using rate constants and reactions as described in text.

made using N_2O-saturated aqueous solutions in order to maximize the effect of the hydroxyl radical reactions.

The measured decreases in ether concentrations with applied dose are shown in Figure 5. The initial loss of ether concentration followed an exponential-type decay, with total initial ether (50 ppmw) removal occurring by a dose of ~5 kGy. Also shown in Figure 5 are the results of some preliminary computer modeling of the radiolysis of these ethers. The kinetic model used consisted of the full set of water radiolysis reactions and rate constants,[23] the reactions of the hydrated electron and hydrogen atom with N_2O, and the reactions of •OH, e_{aq}^-, and •H with the ethers of this study. No subsequent reactions of the produced ether radicals were considered. The theoretical loss curves show excellent agreement for ETBE and TAME loss. A slight deviation from the experimental measurements is seen for DIPE, however, there is good agreement within the experimental measurement error (±1−2 ppm).

The very good agreement seen between the experimental steady-state measurements and the predictions of this simple kinetic model is somewhat surprising. One would expect that the initial reaction products of ETBE would be equally good at reacting with •OH radicals under these experimental conditions. We are presently performing additional product analyses on these irradiated solutions in order to identify these radiolysis products, and to allow further development of the overall mechanism of free-radical destruction of these ethers in water.

Summary

Absolute rate constants for the reactions of the hydroxyl radical, hydrated electron, and hydrogen atom with ETBE, DIPE, and TAME in water have been determined at room temperature. The hydroxyl radical rate constants are the largest, ($\sim 2 \times 10^9$ dm^3 mol^{-1} s^{-1}), and therefore expected to be the dominant reaction pathway for AOT treatment of ether-contaminated water. Only a minimal contribution from the corresponding hydrated electron ($<10^7$ dm^3 mol^{-1} s^{-1}) and hydrogen atom ($\sim 10^7$ dm^3 mol^{-1} s^{-1}) reactions would be expected to occur.

Acknowledgment. Partial support for this research was provided by the National Science Foundation, under Grant BES 97-29965. Work described herein at the Radiation Laboratory, University of Notre Dame, was supported by the Office of Basic Energy Sciences of the U.S. Department of Energy. Work performed at Argonne National Laboratory was supported by the U.S. Office of Basic Energy Sciences, Division of Chemical Sciences, US-DOE, under Contract No. W-31-109-ENG-38.

References and Notes

(1) *Guidance on Estimating Motor Vehicle Emission Reductions from the Use of Alternative Fuels and Fuel Blends*; Report No. EPA-AA-TSS-PA-87-4; U.S.E.P.A.: Ann Arbor, MI, 1988.
(2) Squillace, P. J.; Pankow, J. F.; Korte, N. E.; Zogorski, J. S. *Environ. Toxicol. Chem.* **1997**, *16*, 1836.
(3) Robles, H.; Schumacher, T. T. In *Preprints of Extended Abstracts, American Chemical Society Division of Environmental Chemistry: 219th ACS National Meeting, San Francisco, CA*, March 2000; p 301.
(4) Salanitro, J. P.; Diaz, L. A.; Willams, M. P.; Wisniewski, H. L. *Appl. Environ. Microbiol.* **1994**, *60*, 2593.
(5) Suflita, J. M.; Mormile, M. *Environ. Sci. Technol.* **1993**, *27*, 976.
(6) Davidson, J. M.; Parsons, R. In *Proceedings of the Petroleum Hydrocarbons and Organic Chemicals in Ground Water: Prevention, Detection and Remediation Conference, Nov 13−15, 1996*; Ground Water Publishing Company: Houston, TX, 1996; p 15.
(7) *Alcohols and Ethers: A Technical Assessment of their Application as Fuels and Fuel Components*; Publ. No. 4261; American Petroleum Institute: Washington, DC, July 1998.
(8) Morse, P. M. *Chem. Eng. News* **1999**, April, 26.
(9) Robbins, G. A.; Wang, S.; Stuart, J. D. *Anal. Chem.* **1993**, *65*, 3113.
(10) Cater, S. R.; Stefan, M. I.; Bolton, J. R.; Safarzadeh-Amiri, A. *Environ. Sci. Technol.* **2000**, *34*, 659.
(11) Peyton, G. R.; Bell, O. J.; Girin, E.; Lefaivre, M. H. *Environ. Sci. Technol.* **1995**, *29*, 1710.
(12) Crittenden, J. C.; Hu, S.; Hand, D. W.; Green, S. A. *Water Res.* **1999**, *33*, 2315.
(13) Cooper, W. J.; et al. Submitted for publication in *Environ. Sci. Technol*.
(14) Whitman, K.; Lyons, S.; Miller, R.; Nett, D.; Treas, P.; Zante, A.; Fessenden, R. W.; Thomas, M. D.; Wang, Y. In *Proceedings of the '95 Particle Accelerator Conference and International Conference on High Energy Accelerators*, Texas; 1996.
(15) Buxton, G. V.; Stuart, C. R. *J. Chem. Soc., Faraday Trans.* **1995**, *91*, 279.
(16) Fessenden, R. W.; Varma, N. C. *Faraday Discuss. Chem. Soc.* **1977**, *63*, 104.
(17) Bartels, D. M.; Craw, M. T.; Han, P.; Trifunac, A. D. *J. Phys. Chem.* **1989**, *93*, 2412.
(18) Han, P.; Bartels, D. M. *Chem. Phys. Lett.* **1989**, *159*, 538.
(19) Han, P.; Bartels, D. M. *J. Phys. Chem.* **1990**, *94*, 7294.
(20) Han, P.; Bartels, D. M. *J. Phys. Chem.* **1992**, *96*, 4899.
(21) Roduner, E.; Bartels, D. M. *Ber. Bunsen-Ges. Phys. Chem.* **1992**, *96*, 1037.
(22) Bartels, D. M.; Mezyk, S. P. *J. Phys. Chem.* **1993**, *97*, 4101.
(23) Buxton, G. V.; Greenstock, C. L.; Helman, W. P.; Ross, A. B. *J. Phys. Chem. Ref. Data* **1988**, *17*, 513.
(24) Capellos, C.; Bielski, B. H. J. *Kinetic Systems: Mathematical Description of Chemical Kinetics in Solution*; Wiley-Interscience: New York, 1972.
(25) Hart, E. J.; Thomas, J. K.; Gordon, S. *Radiat. Res. Suppl.* **1964**, *4*, 74.
(26) Koehler, G.; Solar, S.; Getoff, N.; Holzwarth, A. R.; Schaffner, K. *J. Photochem.* **1985**, *28*, 383.
(27) Neta, P.; Fessenden, R. W.; Schuler, R. H. *J. Phys. Chem.* **1971**, *75*, 1654.
(28) Pimblott, S. M.; LaVerne, J. A. *Radiat. Res.* **1990**, *122*, 12.
(29) LaVerne, J. A.; Pimblott, S. M. *J. Phys. Chem.* **1991**, *95*, 3196.
(30) Pimblott, S. M.; LaVerne, J. A. *Radiat. Res.* **1992**, *129*, 265.
(31) Pimblott, S. M.; LaVerne, J. A. *J. Phys. Chem.* **1992**, *96*, 8904.
(32) Schuchmann, M. N.; von Sonntag, C. *Z. Naturforsch.* **1986**, *42b*, 495.
(33) Eibenberger, J. Ph.D. Thesis, University of Vienna, Austria, 1980.
(34) Karpel Vel Leitner, N.; Papailhou, A.-L.; Croue, J.-P.; Peyrot, J.; Dore, M. *Ozone Sci. Eng.* **1994**, *16*, 41.
(35) Thomas, J. K. *Trans. Faraday Soc.* **1965**, *61*, 702.
(36) Wallington, T. J.; Dagaut, P.; Kurylo, M. J. *J. Phys. Chem.* **1988**, *92*, 5024.
(37) Wallington, T. J.; Dagaut, P.; Liu, R.; Kurylo, M. J. *Environ. Sci. Technol.* **1988**, *22*, 842.
(38) Wallington, T. J.; Dagaut, P.; Liu, R.; Kurylo, M. J. *Int. J. Chem. Kinet.* **1988**, *20*, 541.
(39) Wallington, T. J.; Liu, R.; Dagaut, P.; Kurylo, M. J. *Int. J. Chem. Kinet.* **1988**, *20*, 41.
(40) Notario, A.; Mellouki, A.; Le Bras, G. *Int. J. Chem. Kinet.* **2000**, *32*, 105.